10.24425/acs.2025.153960

Archives of Control Sciences
Volume 35(LXXI), 2025
No. 1, *pages 123–143*

A new chaotic hyperjerk system with a half-line of equilibrium points, its dynamic analysis, multistability, circuit simulation and anti-synchronization via backstepping control

Sundarapandian VAIDYANATHAN, Fareh HANNACHI, Mohamad Afendee MOHAMED, Aceng SAMBAS, Chittineni ARUNA and Repudi RAMESH

In this work, we present a new four-dimensional chaotic hyperjerk system with a half-line of equilibrium points. In the chaos literature, it is well-known that chaotic systems with an infinite number of equilibrium points exhibit *hidden attractors*. Thus, we deduce in this research work that the new chaotic hyperjerk system has hidden attractors. We next study the new chaotic hyperjerk system for a dynamic analysis using bifurcation plots and Lyapunov Exponents (LE) diagrams. We exhibit that the new hyperjerk system has a special property of multistability with coexisting attractors. Using Multisim version 14.2, we carry out an electronic circuit simulation for the proposed 4-D chaotic hyperjerk system with a half-line of equilibrium points. Finally, as an application in control engineering, we apply backstepping control for achieving anti-synchronization of a pair of new chaotic hyperjerk systems taken as master-slave systems, which has important applications in communication systems.

S. Vaidyanathan (corresponding author, e-mail: sundar@veltech.edu.in) is with Centre for Control Systems, Vel Tech University, 400 Feet Outer Ring Road, Avadi, Chennai-600062 Tamil Nadu, India and Faculty of Information and Computing, Universiti Sultan Zainal Abidin Terengganu, Malaysia.

F. Hannachi (e-mail: fareh.hannachi@univ-tebessa.dz) is with Department of Management Sciences, Echahid Cheikh Larbi Tebessi University, Route de Constantine, 12022, Tebessa, Algeria.

M.A. Mohamed (e-mail: mafendee@unisza.edu.my) is with Faculty of Information and Computing, Universiti Sultan Zainal Abidin, Terengganu, Malaysia.

A. Sambas (e-mails: acengsambas@unisza.edu.my, acengs@umtas.ac.id) is with Faculty of Informatics and Computing, Universiti Sultan Zainal Abidin, Gong Badak, 21300, Terengganu, Malaysia and Department of Mechanical Engineering, Universitas Muhammadiyah Tasikmalaya, Jawa Barat 46196, Indonesia.

C. Aruna (e-mail: aruna.cse@kitsguntur.ac.in) and R. Ramesh (e-mail: ramesh.cse@kitsguntur.ac.in) are with Department of Computer Science and Engineering, KKR & KSR Institute of Technology and Sciences, Vinjanampadu, Vatticherukuru Mandal, Guntur-522017, Andhra Pradesh, India.

Received 28.03.2024.

Key words: chaos, hyperjerk systems, chaotic systems, bifurcation, multistability, circuit simulation, anti-synchronization, backstepping control

1. Introduction

Chaotic dynamical systems with their complex dynamics have several applications in areas such as robotics [1, 2], oscillators [3, 4], memristors [5, 6], fuzzy systems [7, 8], communication systems [9, 10], etc. Chaos theory also has applications in mechanical systems such as jerk systems [11, 12] and hyperjerk systems [13–16], etc.

A *hyperjerk* differential equation of fourth order has the general form

$$\frac{\mathrm{d}^4 p}{\mathrm{d}t^4} = F\left(p(t), \frac{\mathrm{d}p}{\mathrm{d}t}, \frac{\mathrm{d}^2 p}{\mathrm{d}t^2}, \frac{\mathrm{d}^3 p}{\mathrm{d}t^3}\right). \tag{1}$$

If $p(t)$ denotes the displacement of a body, then the first two derivatives $\dfrac{\mathrm{d}p}{\mathrm{d}t}$ and $\dfrac{\mathrm{d}^2 p}{\mathrm{d}t^2}$ represent the *velocity* and *acceleration* of the body. The third order derivative $\dfrac{\mathrm{d}^3 p}{\mathrm{d}t^3}$ is called the *jerk*, while the fourth order derivative $\dfrac{\mathrm{d}^4 p}{\mathrm{d}t^4}$ is called the *hyperjerk*.

In system form, the hyperjerk differential equation (1) can be expressed as

$$\begin{cases} \dot{x} = y, \\ \dot{y} = z, \\ \dot{z} = w, \\ \dot{w} = F(x, y, z, w). \end{cases} \tag{2}$$

In the chaos literature, there is significant interest in the modelling and simulation of chaotic systems with an infinite number of equilibrium points [17]. Such chaotic systems are known to possess hidden chaotic attractors, which have important applications in science and engineering [18–20].

Recently, Sambas *et al.* [15] reported a new chaotic hyperjerk system with a half-line of equilibrium points. By modifying the dynamics of the Sambas hyperjerk system [15], we obtain a new hyperjerk system with more complexity than the Sambas hyperjerk system [15].

We carry out a detailed bifurcation analysis of the new chaotic hyperjerk system with a half-line of equilibrium points. Bifurcation analysis of nonlinear dynamical systems brings out important and intrinsic qualitative properties of the systems [21, 22]. We also design an electronic circuit of the new chaotic hyperjerk system with a half-line of equilibrium points. Electronic circuit designs of chaotic

systems aid in applications of the chaotic systems to real-world applications in science and engineering [23, 24].

As a control application, we invoke backstepping control technique [27] for achieving complete anti-synchronization between a pair of new chaotic hyperjerk systems taken as the *master* and *slave systems*. We remark that anti-synchronization (AS) of chaotic systems is a phenomenon in which the state vectors of the synchronized systems have the same amplitude but opposite signs as those of the driving system. Thus, for anti-synchronization of chaotic systems, the sums of the respective signals of the master and slave systems are expected to converge to zero asymptotically with time [25, 26]. Backstepping control method is a popular control strategy for asymptotically stabilizing or synchronizing chaotic dynamical systems [27]. The main advantage of the backstepping control approach is that it follows a systematic procedure in order to obtain the design of the stabilizing controller for driving the synchronization error to zero [28–30].

2. Mathematical modelling of the new hyperjerk system with a half-line of equilibrium points

In [15], Sambas *et al.* (2024) derived a new 3-D chaotic hyperjerk system with the dynamics

$$\begin{cases} \dot{x} = y, \\ \dot{y} = z, \\ \dot{z} = w, \\ \dot{w} = -x - |x| - ay - bw - xz. \end{cases} \tag{3}$$

We set $X = (x, y, z, w)$ to denote the state of the Sambas system (3).

We suppose that a and b are positive constants in the Sambas system (3).

Sambas et al. [15] showed that the system (3) is chaotic when $a = 4$ and $b = 2$.

For the initial state $(0.1, 0.2, 0.1, 0.2)$ and $(a, b) = (4, 2)$, the Lyapunov exponents (LE) of the 4-D Sambas system (3) are determined for $T = 1E4$ seconds in MATLAB as follows:

$$L_1 = 0.1265, \quad L_2 = 0, \quad L_3 = -0.7330, \quad L_4 = -13939. \tag{4}$$

The equilibrium points of the Sambas hyperjerk system (3) are found by solving the equations:

$$y = 0, \tag{5a}$$

$$z = 0, \tag{5b}$$

$$w = 0, \tag{5c}$$

$$-x - |x| - ay - bw - xz = 0. \tag{5d}$$

From (5a), (5b) and (5c), we see that $y = z = w = 0$.

Hence, (5d) simplifies as $x + |x| = 0$.

Thus, the Sambas hyperjerk system (3) consists of the equilibrium points given by the set

$$S = \{(x, y, z, w) : x + |x| = 0, y = 0, z = 0, w = 0\}. \tag{6}$$

When $x \geqslant 0$, $|x| = x$ and the equation $x + |x| = 0$ has the unique solution $x = 0$.

When $x < 0$, $|x| = -x$ and the equation $x + |x| = 0$ is readily satisfied.

Hence, we can simplify the equilibrium set S for the Sambas hyperjerk system (3) as

$$S = \{(x, y, z, w) : x \leqslant 0, y = 0, z = 0, w = 0\} \tag{7}$$

which is the half-line consisting of the non-positive x-axis in $\mathbb{R}^4$.

In this research work, we obtain a new chaotic hyperjerk system by introducing two quadratic nonlinearities in the hyperjerk dynamics (3).

Thus, we propose the following hyperjerk dynamics

$$\begin{cases} \dot{x} = y, \\ \dot{y} = z, \\ \dot{z} = w, \\ \dot{w} = -x - |x| - ay - bw - xz + cz^2 + pyz, \end{cases} \tag{8}$$

where $X = (x, y, z, w)$ is the state and a, b, c, p are positive parameters.

In this research work, we shall show that the new hyperjerk system (8) is chaotic for the values

$$a = 4, \quad b = 2, \quad c = 0.1, \quad p = 0.2. \tag{9}$$

For the initial state $(0.1, 0.2, 0.1, 0.2)$ and $(a, b, c, p) = (4, 2, 0.1, 0.2)$, the Lyapunov exponents (LE) of the new 4-D hyperjerk system (8) are determined for $T = 1E4$ seconds in MATLAB as follows:

$$L_1 = 0.2035, \quad L_2 = 0, \quad L_3 = -0.7445, \quad L_4 = -1.4255. \tag{10}$$

The equilibrium points of the new hyperjerk system (8) are found by solving the equations:

$$y = 0, \tag{11a}$$

$$z = 0, \tag{11b}$$

$$w = 0, \tag{11c}$$

$$-x - |x| - ay - bw - xz + cz^2 + pyz = 0. \tag{11d}$$

From (11a), (11b) and (11c), we see that $y = z = w = 0$.

Hence, (11d) simplifies as $x + |x| = 0$.

Thus, the new hyperjerk system (8) consists of the equilibrium points given by the set

$$S = \{(x, y, z, w) : x + |x| = 0,\ y = 0,\ z = 0,\ w = 0\}. \tag{12}$$

When $x \geqslant 0$, $|x| = x$ and the equation $x + |x| = 0$ has the unique solution $x = 0$.

When $x < 0$, $|x| = -x$ and the equation $x + |x| = 0$ is readily satisfied.

Hence, we can simplify the equilibrium set S for the new hyperjerk system (8) as

$$S = \{(x, y, z, w) :\ x \leqslant 0, y = 0, z = 0, w = 0\} \tag{13}$$

which is the half-line consisting of the non-positive x-axis in $\mathbb{R}^4$.

Comparing the equations (4) and (10), we make the deduction that the maximal Lyapunov exponent (MLE) of the new hyperjerk system is $L_1 = 0.2035$ which is greater than the MLE of the Sambas hyperjerk system (1) obtained as $L_1 = 0.1265$. Thus, the new hyperjerk system (8) exhibits more complexity than the Sambas hyperjerk system (3).

Figures 1–4 show the 2-D phase plots of the new hyperjerk system (8) in (x, y), (y, z), (z, w) and (x, w) planes, respectively.

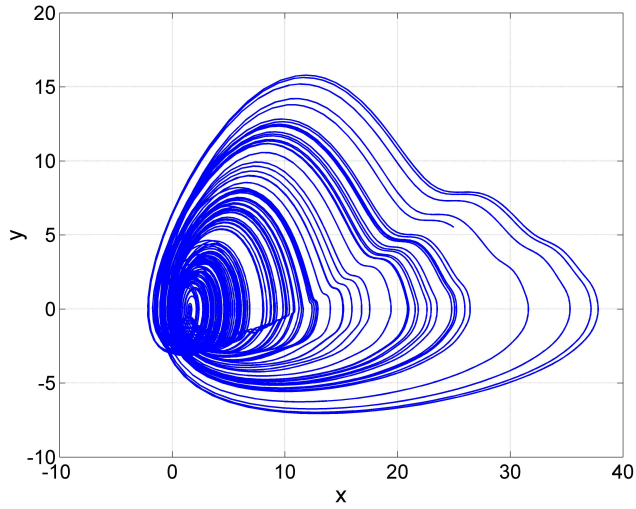

Figure 1: 2-D plot of the new hyperjerk system (8) for $X(0) = (0.1, 0.2, 0.1, 0.2)$ and $(a, b, c, p) = (4, 2, 0.1, 0.2)$ in (x, y) plane

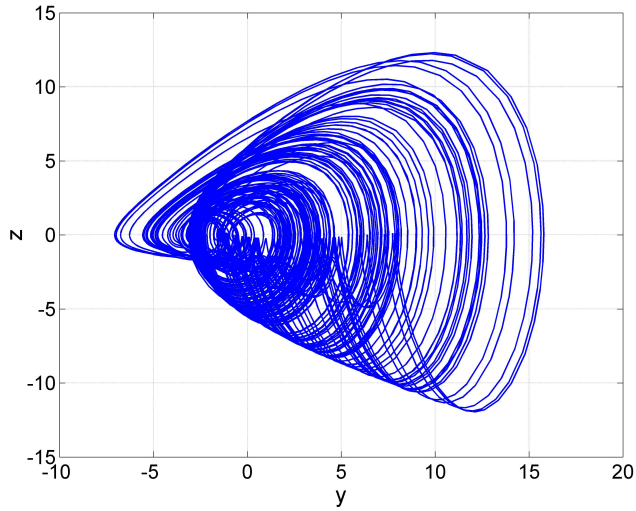

Figure 2: 2-D plot of the new hyperjerk system (8) for $X(0) = (0.1, 0.2, 0.1, 0.2)$ and $(a, b, c, p) = (4, 2, 0.1, 0.2)$ in (y, z) plane

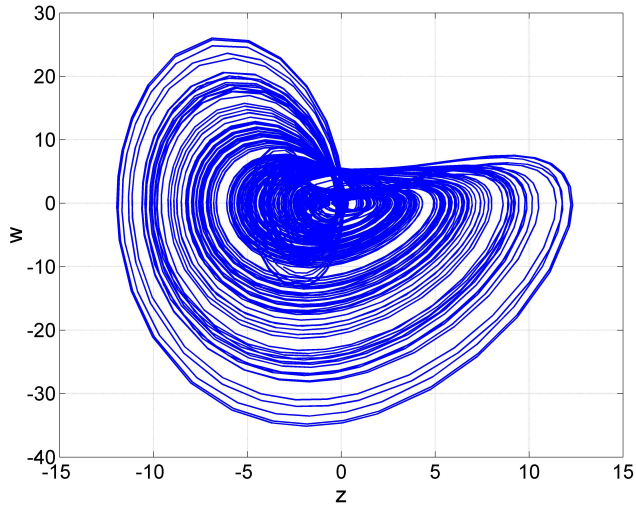

Figure 3: 2-D plot of the new hyperjerk system (8) for $X(0) = (0.1, 0.2, 0.1, 0.2)$ and $(a, b, c, p) = (4, 2, 0.1, 0.2)$ in (z, w) plane

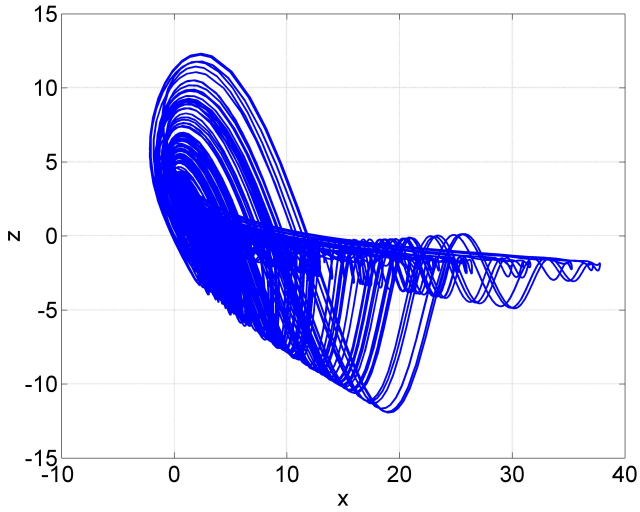

Figure 4: 2-D plot of the new hyperjerk system (8) for $X(0) = (0.1, 0.2, 0.1, 0.2)$ and $(a, b, c, p) = (4, 2, 0.1, 0.2)$ in (x, z) plane

3. Bifurcation analysis of the New Hyperjerk System with a half-line of equilibrium points

In this section, we investigate numerically the dynamical behavior of the new hyperjerk system (8) with a half-line of equilibrium points using the LE spectrum and bifurcation diagrams.

3.1. Varying the parameter a

Figure 5 shows the Lyapunov exponents (LE) spectrum and the bifurcation diagram of the new 4-D chaotic hyperjerk system (8) with respect to parameter a.

We fix the values the parameters: b, c, p as: $(b, c, p) = (2, 0.1, 0.2)$.

We can identify the dynamic behavior of the new hyperjerk system (8) when the parameter a varies in the range $[3.96, 5]$ as follows:

Let $a \in [3.96, 5]$. We define:

$A = [3.96, 4.29) \cup (4.29, 4.55) \cup (4.56, 4.71) \cup (4.77, 4.873)$,

$B = [4.55, 4.56] \cup [4.71, 4.77] \cup [4.873, 5] \cup \{4.29\}$.

When $a \in A$, we can see from Figure 5 that the new hyperjerk system (8) has only one positive Lyapunov exponent ($L_1 > 0$) and one zero Lyapunov exponent ($L_2 = 0$) and two negative Lyapunov exponents ($L_{3,4} < 0$). Thus, the hyperjerk system (8) is chaotic and generates a chaotic attractor in this range of parameter a.

The LE values of the hyperjerk system (8) when $a = 4.05$ are:

$$L_1 = 0.1284, \quad L_2 = 0, \quad L_3 = -0.6929, \quad L_4 = -1.4370. \tag{14}$$

The LE values of the hyperjerk system (8) when $a = 4.25$ are:

$$L_1 = 0.1319, \quad L_2 = 0, \quad L_3 = -0.6510, \quad L_4 = -1.4820. \tag{15}$$

The LE values of the hyperjerk system (8) when $a = 4.61$ are:

$$L_1 = 0.04029, \quad L_2 = 0, \quad L_3 = -0.5663, \quad L_4 = -1.4080. \tag{16}$$

When $a \in B$, we can see from Figure 5 that the system (8) has only one zero Lyapunov exponent ($L_1 = 0$) and three negative Lyapunov exponents ($L_{2,3,4} < 0$).

Thus, for values of $a \in B$, the hyperjerk system (8) is periodic and generates a periodic attractor.

The LE values of the hyperjerk system (8) when $a = 4.29$ are:

$$L_1 = 0, \quad L_2 = -0.04562, \quad L_3 = -0.4740, \quad L_4 = -1.4830. \tag{17}$$

The LE values of the hyperjerk system (8) when $a = 4.75$ are:

$$L_1 = 0, \quad L_2 = -0.04562, \quad L_3 = -0.4740, \quad L_4 = -1.4830. \tag{18}$$

The LE values of the hyperjerk system (8) when $a = 5$ are:

$$L_1 = 0, \quad L_2 = -0.03708, \quad L_3 = -0.4960, \quad L_4 = -1.470. \tag{19}$$

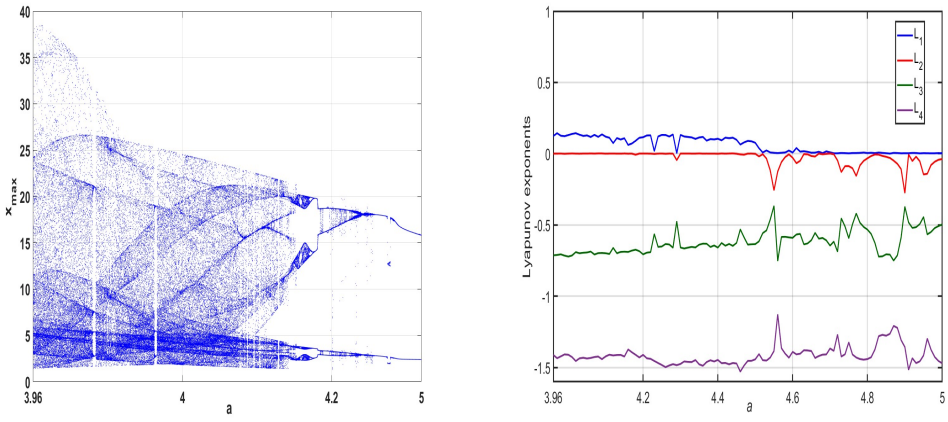

(a) Bifurcation plot (b) LE spectrum

Figure 5: Bifurcation diagram and LE Spectrum for the hyperjerk system (8) when a varies in $[3.96, 5]$ and $(b, c, p) = (2, 0.1, 0.2)$

3.2. Varying the parameter b

Figure 6 shows the Lyapunov exponents (LE) spectrum and the bifurcation diagram of the new 4-D chaotic hyperjerk system (8) with respect to parameter b.

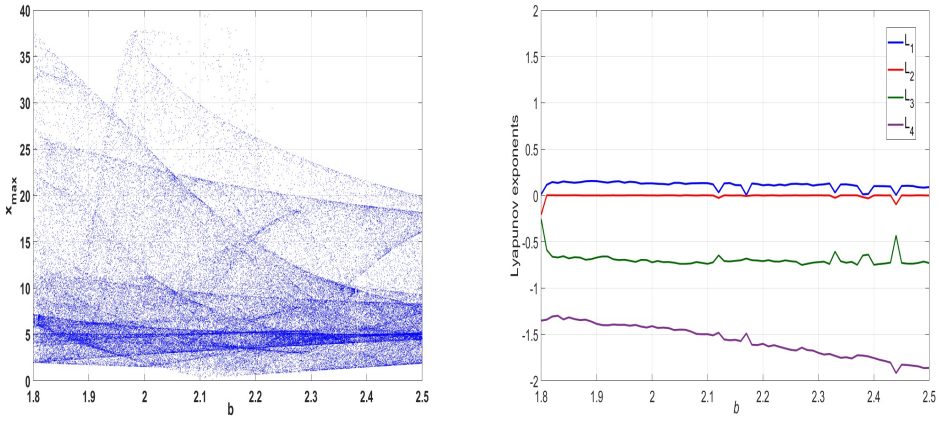

(a) Bifurcation plot (b) LE spectrum

Figure 6: Bifurcation diagram and LE Spectrum for the hyperjerk system (8) when b varies in $[1.8, 2.5]$ and $(a, c, p) = (4, 0.1, 0.2)$

We fix the values the parameters: a, c, p as: $(a, c, p) = (4, 0.1, 0.2)$.

We vary the parameter b in the range $[1.8, 2.5]$.

We can see from Fig. 6 that the hyperjerk system (8) has at least one positive Lyapunov exponent ($L_1 > 0$). Thus, the hyperjerk system (8) is chaotic and generates a chaotic attractor in this range of parameter b.

The LE values of the hyperjerk system (8) when $b = 1.9$ are:

$$L_1 = 0.1548, \quad L_2 = 0, \quad L_3 = -0.67, \quad L_4 = -1.385. \tag{20}$$

The LE values of the hyperjerk system (8) when $b = 2.05$ are:

$$L_1 = 0.1363, \quad L_2 = 0, \quad L_3 = -0.7377, \quad L_4 = -1.4480. \tag{21}$$

The LE values of the hyperjerk system (8) when $b = 2.32$ are:

$$L_1 = 0.1299, \quad L_2 = 0, \quad L_3 = -0.7397, \quad L_4 = -1.7110. \tag{22}$$

3.3. Varying the parameter c

Figure 7 shows the Lyapunov exponents spectrum and the bifurcation diagram of the new 4-D chaotic hyperjerk system (8) with respect to parameter c.

We fix the values the parameters: a, b, p as: $(a, b, p) = (4, 2, 0.2)$.

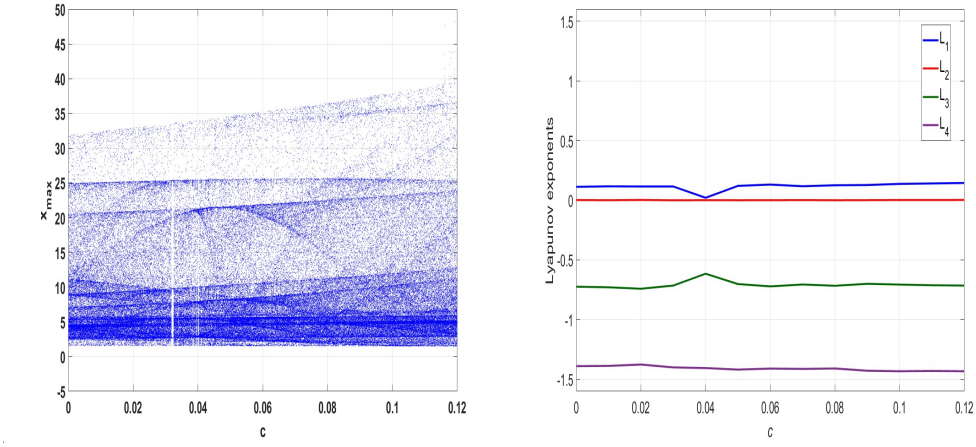

(a) Bifurcation plot (b) LE spectrum

Figure 7: Bifurcation diagram and LE Spectrum for the hyperjerk system (8) when c varies in $[0, 0.12]$ and $(a, b, p) = (4, 2.0.2)$

We vary the parameter c in the range $[0, 0.12]$.

We can see from Figure 7 that the hyperjerk system (8) has at least one positive Lyapunov exponent ($L_1 > 0$). Thus, the hyperjerk system (8) is chaotic and generates a chaotic attractor in this range of parameter c.

The LE values of the hyperjerk system (8) when $c = 0.06$ are:

$$L_1 = 0.1313, \quad L_2 = 0, \quad L_3 = -0.7215, \quad L_4 = -1.41. \tag{23}$$

The LE values of the hyperjerk system (8) when $c = 0.09$ are:

$$L_1 = 0.1275, \quad L_2 = 0, \quad L_3 = -0.7, \quad L_4 = -1.4280. \tag{24}$$

The LE values of the hyperjerk system (8) when $c = 0.12$ are:

$$L_1 = 0.1448, \quad L_2 = 0, \quad L_3 = -0.7147, \quad L_4 = -1.4320. \tag{25}$$

3.4. Varying the parameter p

Figure 8 shows the Lyapunov exponents spectrum and the bifurcation diagram of the new 4-D chaotic hyperjerk system (8) with respect to parameter p.

We fix the values the parameters: a, b, c as: $(a, b, c) = (4, 2, 0.1)$. We vary the parameter p in the range $[0, 0.24]$. we can see from Figure 8 that the hyperjerk system (8) has at least one positive Lyapunov exponent ($L_1 > 0$).

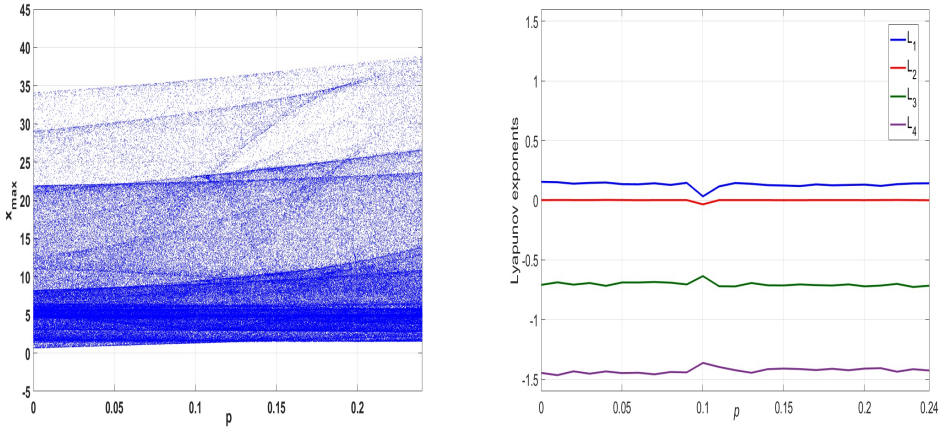

(a) Bifurcation plot (b) LE spectrum

Figure 8: Bifurcation diagram and LE Spectrum for the hyperjerk system (8) when p varies in $[0, 0.24]$ and $(a, b, c) = (4, 2.0.1)$

Thus, the hyperjerk system (8) is chaotic and generate a chaotic attractor in this range of parameter p.

The LE values of the hyperjerk system (8) when $p = 0.04$ are:

$$L_1 = 0.1484, \quad L_2 = 0, \quad L_3 = -0.7170, \quad L_4 = -1.4340. \tag{26}$$

The LE values of the hyperjerk system (8) when $p = 0.13$ are:

$$L_1 = 0.1375, \quad L_2 = 0, \quad L_3 = -0.6932, \quad L_4 = -1.4450. \tag{27}$$

The LE values of the hyperjerk system (8) when = 0.24 are:

$$L_1 = 0.1419, \quad L_2 = 0, \quad L_3 = -0.7157, \quad L_4 = -1.4260. \tag{28}$$

4. Multistability in the new chaotic hyperjerk system

To enhance the examination of coexistence attractors and other system characteristics, introducing a disturbance to the initial conditions is essential, while maintaining constant system parameters. Figures 9 and 10 show the dynamic behavior of the hyperjerk system (8) with coexistence of attractors for different initial conditions and same values of system parameters.

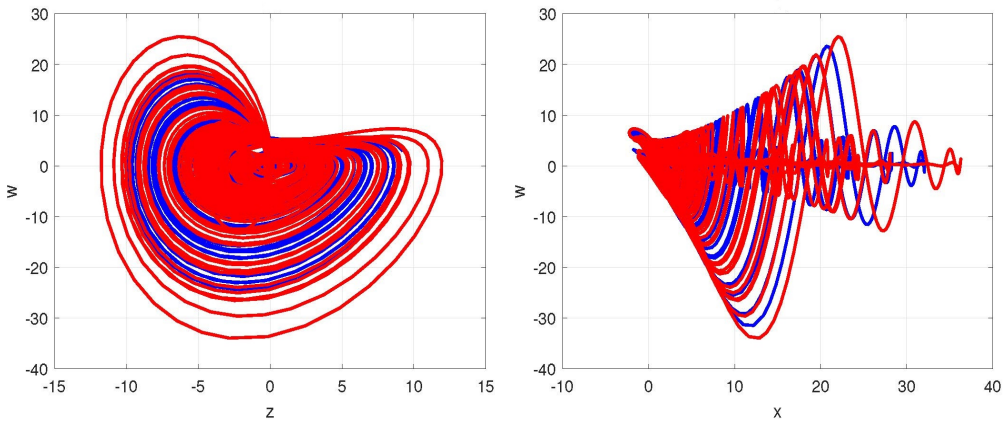

(a) (z, w) plot (b) (x, w) plot

Figure 9: Coexistence of two chaotic attractors for the hyperjerk system (8) with different initial values where $a = 4, b = 2, c = 0.1, q = 0.2$: (a-b) The initial states are chosen as $X_0 = (0.1, 0.2, 0.1, 0.2)$ (blue orbit) and $X_1 = (0.1, 0.2, 0.1, 0.5)$ (red orbit)

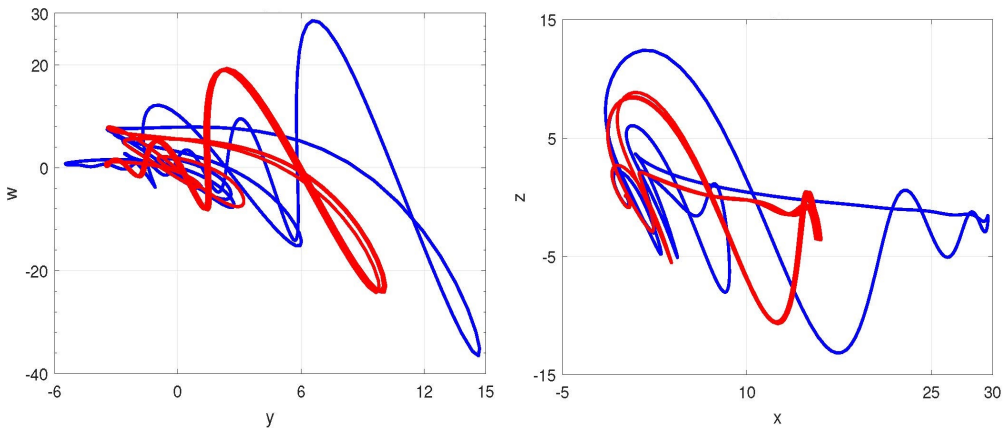

(a) (y, w) plot (b) (x, z) plot

Figure 10: Coexistence of two periodic attractors for the hyperjerk system (8) with different initial values where $a = 5, b = 2, c = 0.1, q = 0.2$: (a-b) The initial states are chosen as $X_0 = (0.1, 0.2, 0.1, 0.2)$ (blue orbit) and $X_1 = (0.1, 0.2, 0.1, 0.5)$ (red orbit).

5. Circuit simulation of the new chaotic hyperjerk system

In this section, the new 4D chaotic hyperjerk system (8) is realized by the NI Multisim 14.2 platform. The electronic circuit design of the 4D hyperjerk chaotic circuit (29) is shown in Figure 11 in which TLO82CD is selected as OPAMP and the multipliers are of type AD633.

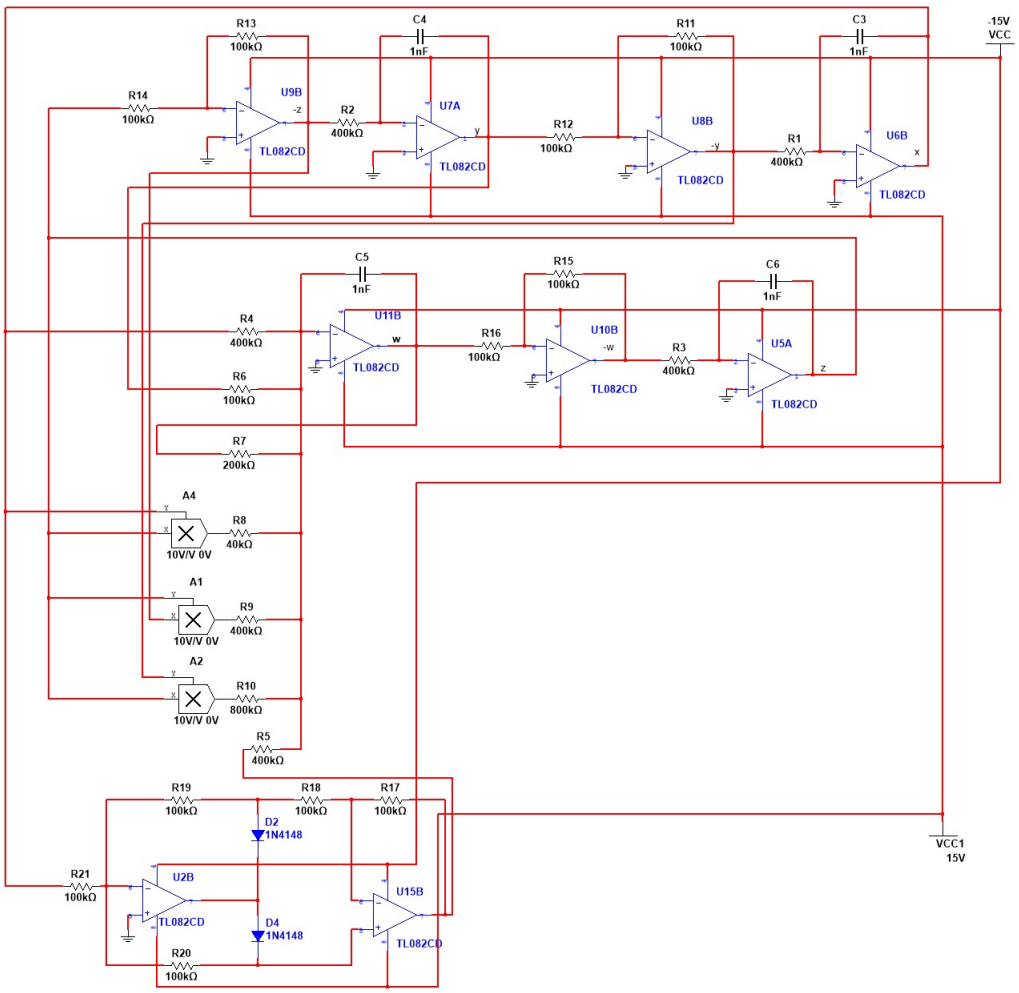

Figure 11: Circuit design of the new chaotic 4D hyperjerk system (29)

Using Kirchhoff's electrical circuit laws, we derive the circuit model for the new chaotic 4D hyperjerk system (8) as follows:

$$\begin{cases} \dot{x} = \dfrac{1}{R_1C_1}y, \quad \dot{y} = \dfrac{1}{R_2C_2}z, \quad \dot{z} = \dfrac{1}{R_3C_3}w, \\ \dot{w} = -\dfrac{1}{R_4C_4}x - \dfrac{1}{R_5C_4}|x| - \dfrac{1}{R_6C_4}y - \dfrac{1}{R_7C_4}w - \dfrac{1}{10R_8C_4}xz \\ \qquad + \dfrac{1}{10R_9C_4}z^2 + \dfrac{1}{10R_{10}C_4}yz. \end{cases} \tag{29}$$

Here x, y, z, w are the voltages across the capacitors, $C1, C2, C3, C3$, respectively. The values of components in the circuit are selected as follow:

$$R_1 = R_2 = R_3 = R_4 = R_5 = R_9 = 400\ \text{k}\Omega,\ \ R_7 = 200k\Omega, R_8 = 40\ \text{k}\Omega, \tag{30}$$

$$R_6 = R_{11} = R_{12} = R_{13} = R_{14} = R_{15} = 100\ \text{k}\Omega, \tag{31}$$

$$R_{16} = R_{17} = R_{18} = R_{19} = R_{20} = R_{21} = 100\ \text{k}\Omega, \tag{32}$$

$$C_1 = C_2 = C_3 = 1\ \text{nF}. \tag{33}$$

Multisim outputs of the hyperjerk circuit (29) via oscilloscope XSC1 are presented in Figure 12.

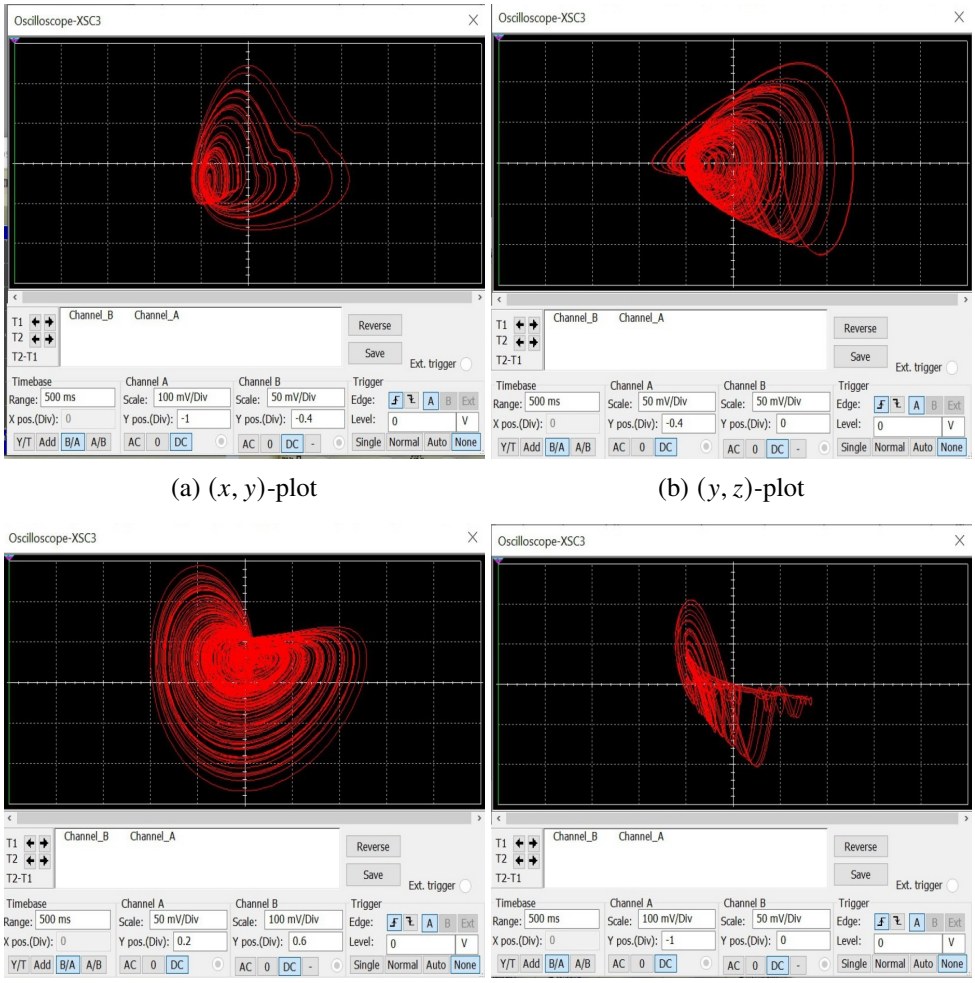

(a) (x, y)-plot (b) (y, z)-plot

(c) (z, w)-plot (d) (x, z)-plot

Figure 12: MultiSim outputs of the new hyperjerk circuit (29) via oscilloscope XSC1

Multisim outputs of the hyperjerk circuit (29) via Tektronix oscilloscope are presented in Figure 13.

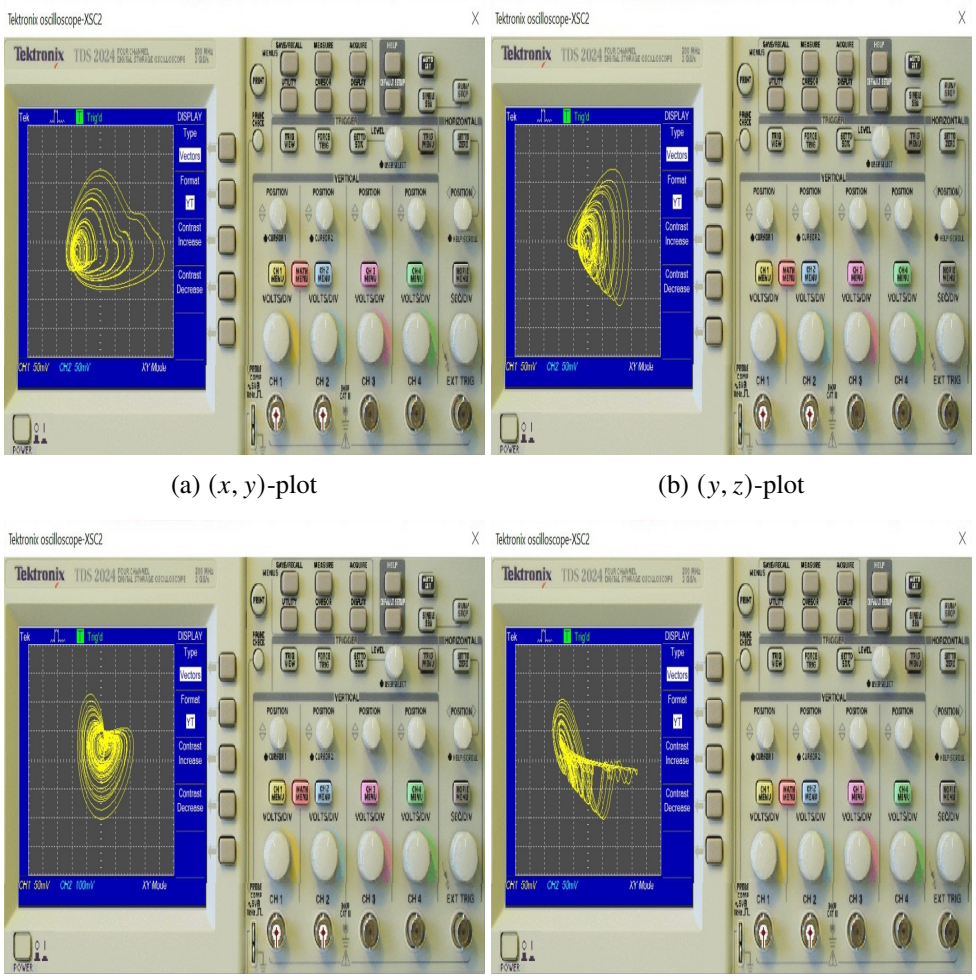

(a) (x, y)-plot (b) (y, z)-plot

(c) (z, w)-plot (d) (x, z)-plot

Figure 13: MultiSim outputs of the new hyperjerk circuit (29) via Tektronix oscilloscope

6. Anti-synchronization of the new chaotic hyperjerk systems via backstepping control

In this section, we invoke backstepping control technique [27] for achieving complete anti-synchronization between a pair of new chaotic hyperjerk systems taken as the *master* and *slave systems*. We remark that anti-synchronization (AS) of chaotic systems is a phenomenon in which the state vectors of the synchro-

nized systems have the same amplitude but opposite signs as those of the driving system. Thus, for anti-synchronization of chaotic systems, the sums of the respective signals of the master and slave systems are expected to converge to zero asymptotically with time [25, 26].

The master hyperjerk system is taken as the new chaotic hyperjerk system with a half-line of equilibrium points given by

$$\begin{cases} \dot{x}_1 = y_1\,, \\ \dot{y}_1 = z_1\,, \\ \dot{z}_1 = w_1\,, \\ \dot{w}_1 = -x_1 - |x_1| - a y_1 - b w_1 - x_1 z_1 + c z_1^2 + p y_1 z_1\,. \end{cases} \tag{34}$$

We denote the state of the 4-D master hyperjerk system (34) as $X = (x_1, y_1, z_1, w_1)$.

The slave hyperjerk system is taken as the new controlled chaotic hyperjerk system

$$\begin{cases} \dot{x}_2 = y_2\,, \\ \dot{y}_2 = z_2\,, \\ \dot{z}_2 = w_2\,, \\ \dot{w}_2 = -x_2 - |x_2| - a y_2 - b w_2 - x_2 z_2 + c z_2^2 + p y_2 z_2 + Q(t). \end{cases} \tag{35}$$

We denote the state of the 4-D slave hyperjerk system (35) as $Y = (x_2, y_2, z_2, w_2)$.

Also, Q is the active backstepping control which is to be determined using backstepping control theory.

The anti-synchronization chaos error between the master and slave hyperjerk systems is defined as follows:

$$\begin{cases} e_x = x_2 + x_1\,, \\ e_y = y_2 + y_1\,, \\ e_z = z_2 + z_1\,, \\ e_w = w_2 + w_1\,. \end{cases} \tag{36}$$

The anti-synchronization error dynamics is calculated as follows:

$$\begin{cases} \dot{e}_x = e_y\,, \\ \dot{e}_y = e_z\,, \\ \dot{e}_z = e_w\,, \\ \dot{e}_w = -e_x - a e_y - b e_w - |x_2| - |x_1| - x_1 z_1 - x_2 z_2 \\ \qquad + c\left(z_1^2 + z_2^2\right) + p(y_1 z_1 + y_2 z_2) + Q(t). \end{cases} \tag{37}$$

We state and prove the main control result of this section.

Theorem 1. *The active backstepping control law stated by*

$$Q(t) = -4e_x - (10-a)e_y - 9e_z - (4-b)e_w + |x_1| + |x_2| + x_1z_1 + x_2z_2 - c\left(z_1^2 + z_2^2\right) - p(y_1z_1 + y_2z_2) - K\eta_4\,, \tag{38}$$

where $K > 0$ and $\eta_4 = 3e_x + 5e_y + 3e_z + e_w$, achieves global anti-synchronization between the trajectories of the 4D chaotic hyperjerk systems (34) and (35) for all values of $X(0), Y(0) \in \mathbb{R}^4$.

Proof. For the control design, we start with the Lyapunov function

$$V_1(\eta_x) = \frac{1}{2}\eta_1^2\,, \tag{39}$$

where

$$\eta_1 = e_x\,. \tag{40}$$

Differentiating V_1 with respect to t along the error system (37), we get

$$\dot{V}_1 = \eta_1\dot{\eta}_1 = -\eta_1^2 + \eta_1(e_x + e_y). \tag{41}$$

We define

$$\eta_2 = e_x + e_y \tag{42}$$

Using (42), we simplify (39) as

$$\dot{V}_1 = -\eta_1^2 + \eta_1\eta_2\,. \tag{43}$$

We proceed next with defining the Lyapunov function

$$V_2(\eta_1, \eta_2) = V_1(\eta_1) + \frac{1}{2}\eta_2^2 = \frac{1}{2}\eta_1^2 + \frac{1}{2}\eta_2^2 \tag{44}$$

Differentiating V_2 with respect to t along the error system (37), we get

$$\dot{V}_2 = -\eta_x^2 - \eta_y^2 + \eta_y(2e_x + 2e_y + e_z) \tag{45}$$

We define

$$\eta_3 = 2e_x + 2e_y + e_z \tag{46}$$

Using (46), we simplify (45) as

$$\dot{V}_2 = -\eta_1^2 - \eta_2^2 + \eta_2\eta_3\,. \tag{47}$$

Next, we define the Lyapunov function

$$V_3(\eta_1, \eta_2, \eta_3) = V_2(\eta_x, \eta_y) + \frac{1}{2}\eta_3^2 = \frac{1}{2}(\eta_1^2 + \eta_2^2 + \eta_3^2). \tag{48}$$

Differentiating V_3 with respect to t along the error system (37), we get

$$\dot{V}_3 = -\eta_1^2 - \eta_2^2 - \eta_3^2 + \eta_3(3e_x + 5e_y + 3e_z + e_w) \tag{49}$$

We define

$$\eta_4 = 3e_x + 5e_y + 3e_z + e_w \tag{50}$$

Using (50), we simplify (49) as

$$\dot{V}_3 = -\eta_1^2 - \eta_2^2 - \eta_3^2 + \eta_4\eta_4 \tag{51}$$

Finally, we define the quadratic Lyapunov function

$$V(\eta_1, \eta_2, \eta_3, \eta_4) = V_3(\eta_1, \eta_2, \eta_3) + \frac{1}{2}\, e_4^2 = \frac{1}{2}\, e_1^2 + \frac{1}{2}\, e_2^2 + \frac{1}{2}\, e_3^2 + \frac{1}{2}\, e_4^2 \tag{52}$$

Differentiating V with respect to t, we get

$$\dot{V} = -\eta_1^2 - \eta_2^2 - \eta_3^2 - \eta_4^2 + \eta_4 Z, \tag{53}$$

where

$$Z = \eta_3 + \eta_4 + \dot{\eta}_4\,. \tag{54}$$

Simplifying the expression in (54), we get

$$\begin{aligned} Z = {} & 4e_x + (10 - a)e_y + 9e_z + (4 - b)e_w - |x_1| - |x_2| - x_1 z_1 \\ & - x_2 z_2 + c\left(z_1^2 + z_2\right) + p(y_1 z_1 + y_2 z_2) + Q(t). \end{aligned} \tag{55}$$

Substituting Q from Eq. (38) into (55), we get

$$Z = -K\eta_4\,. \tag{56}$$

Using (56) and (53), we get

$$\dot{V} = -\eta_1^2 - \eta_2^2 - \eta_3^2 - (1 + K)\eta_4^2\,. \tag{57}$$

From (57), $\dot{V}$ is negative definite on $\mathbb{R}^4$.

Consequently, by Lyapunov stability theory, $(e_x(t), e_y(t), e_z(t), e_w(t)) \to 0$ as $t \to \infty$ for all values of the initial conditions $X(0), Y(0) \in \mathbb{R}^4$.

This completes the proof.

For computer simulations, we take the parameter values as in the chaotic case, *viz.* $(a, b, c, p) = (4, 2, 0.1, 0.2)$.

We choose the feedback gain K as $K = 25$.

We take the initial state of the master system (34) as $X(0) = (3.1, 2.4, 4.8, 5.6)$

We take the initial state of the slave system (35) as $Y(0) = (5.9, 1.3, 6.4, 7.2)$.

Figure 14 shows the asymptotic convergence of the anti-synchronization error $e_x(t)$, $e_y(t)$, $e_z(t)$ and $e_w(t)$ between the master system (34) and the slave system (35).

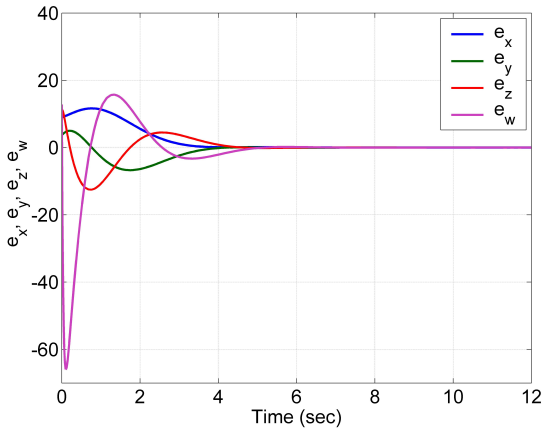

Figure 14: Time-plot of the anti-synchronization errors between the master system (34) and the slave system (35)

7. Conclusions

In this research work, we presented a new 4-D chaotic hyperjerk system with a half-line of equilibrium points. In the chaos literature, it is well-known that chaotic systems with an infinite number of equilibrium points exhibit *hidden attractors*. Thus, we deduced that the new hyperjerk system exhibits hidden chaotic attractors. We presented a detailed study of the new chaotic hyperjerk system for a dynamic analysis using bifurcation plots and Lyapunov Exponents (LE) diagrams. We showed that the new hyperjerk system has a special property of multistability with coexisting attractors. Using Multisim version 14.2, we carried out an electronic circuit simulation for the proposed 4-Dl chaotic hyperjerk system with a half-line of equilibrium points, which will be very useful for practical engineering applications. Finally, as an application in control engineering, we applied active backstepping control for achieving anti-synchronization of a pair of new chaotic hyperjerk systems taken as master-slave systems, which has important applications in communication systems.

References

[1] E. Petavratzis, C. Volos and I. Stouboulos: Experimental study of terrain coverage of an autonomous chaotic mobile robot. *Integration,* **90**(5), (2023), 104–114. DOI: 10.1016/j.vlsi.2023.01.010

[2] A.P. Singh, G. Kumar, G.S. Dhillon and H. Taneja: Hybridization of chaos theory and dragonfly algorithm to maximize spatial area coverage of swarm robots. *Evolutionary Intelligence,* **17**(3), (2024), 1327–1340. DOI: 10.1007/s12065-023-00823-5

[3] K. Huang, C. Li, X. Cen and G. Chen: Constructing chaotic oscillators with memory components. *Chaos, Solitons and Fractals,* **183** (2024). DOI: 10.1016/j.chaos.2024.114917

[4] P. Durairaj, K. Premalatha, S. Kanagaraj, Z. Zheng and K. Rajagopal: Emergence of nonchaotic bursting extreme events in a quadratic jerk oscillator. *Chaos, Solitons and Fractals,* **185** (2024). DOI: 10.1016/j.chaos.2024.115083

[5] J. Fang, J. Wang, N. Fang and Y. Jiang: Design and analysis of a group of correlative and switchable dual memristor hyperchaotic systems. *Journal of Nonlinear Mathematical Physics,***31**(1), (2024). DOI: 10.1007/s44198-024-00204-1

[6] Q. Lai and S. Guo: Heterogeneous coexisting attractors, large-scale amplitude control and finite-time synchronization of central cyclic memristive neural networks. *Neural Networks,* **178** (2024). DOI: 10.1016/j.neunet.2024.106412

[7] R. Abinandhitha, R. Sakthivel, S. Anandhi and O.M. Kwon: Composite resilient reliable control for nonlinear chaotic semi-Markov jump fuzzy systems with multi-source disturbances. *Engineering Applications of Artificial Intelligence,* **133** (2024). DOI: 10.1016/j.engappai.2024.108121

[8] L. Hu, X. Xu, W. Ren and M. Han: Hierarchical evolving fuzzy system: A method for multidimensional chaotic time series online prediction. *IEEE Transactions on Fuzzy Systems,* **32**(6), (2024), 3329–3341. DOI: 10.1109/TFUZZ.2023.3348847

[9] J. Zhang, J. Bi, Y. Guo and P. Wang: Dynamical analysis and circuit realization of a high complexity fourth-order double-wing chaotic system with transient chaos and its application in image encryption. *Physica Scripta,* **99**(7), (2024). DOI: 10.1088/1402-4896/ad564d

[10] F.Q. Meng and G. Wu: A color image encryption and decryption scheme based on extended DNA coding and fractional-order 5D hyper-chaotic system. *Expert Systems with Applications,* **254** (2024). DOI: 10.1016/j.eswa.2024.124413

[11] S. Yan, J. Wang and L. Li: Analysis of a new three-dimensional jerk chaotic system with transient chaos and its adaptive backstepping synchronous control. *Integration,* **98** (2024). DOI: 10.1016/j.vlsi.2024.102210

[12] C. Li, A. Akgul, L. Bi, Y. Xu and C. Zhang: A chaotic jerk oscillator with interlocked offset boosting. *European Physical Journal Plus,* **139**(3), (2024). DOI: 10.1140/epjp/s13360-024-05040-2

[13] R. Kengne, J.T. Mbe, J. Fotsing, A.B. Mezatio, F.J. Ntsafack Manekeng and R. Tchitnga: Dynamics and synchronization of a novel 4D-hyperjerk autonomous chaotic system with a Van der Pol nonlinearity. *Zeitschrift fur Naturforschung - Section A Journal of Physical Sciences,* **78**(9), (2023), 801–821. DOI: 10.1515/zna-2023-0063

[14] E. Zambrano-Serrano and A. Anzo-Hernandez: A novel antimonotic hyperjerk system: Analysis, synchronization and circuit design. *Physica D: Nonlinear Phenomena,* **424** (2021). DOI: 10.1016/j.physd.2021.132927

[15] A. Sambas, M. Miroslav, S. Vaidyanathan, B. Ovilla-Martinez, E. Tlelo-Cuautle, A.A.A. El-latif, B. Abd-El-Atty, K. Benkouider and T. Bonny: A new hyperjerk system with a half line equilibrium: Multistability, period doubling reversals, antimonotonocity, electronic circuit, FPGA design, and an application to image encryption. *IEEE Access,* **12** (2024), 9177–9194. DOI: 10.1109/ACCESS.2024.3351693

[16] S. Vaidyanathan, I.M. Moroz and A. Sambas: A new hyperjerk dynamical system with hyperchaotic attractor and two saddle-focus rest points exhibiting Hopf bifurcations, its hy-

perchaos synchronisation and circuit implementation. *International Journal of Modelling, Identification and Control,* **33**(4), 299–310. DOI: 10.1504/IJMIC.2019.107481

[17] V.-T. Pham, S. Vaidyanathan, C. Volos and T. Kapitaniak: *Nonlinear Dynamical Systems with Self-Excited and Hidden Attractors.* Springer Verlag, Berlin, 2019.

[18] G. Dou, W. Guo, Z. Li and C. Wang: Dynamics analysis of memristor chaotic circuit with coexisting hidden attractors. *European Physical Journal Plus,* **139**(4), (2024). DOI: 10.1140/epjp/s13360-024-05140-z

[19] A. Tiwari, P.P. Singh and B.K. Roy: A realizable chaotic system with interesting sets of equilibria, characteristics, and its underactuated predefined-time sliding mode control. *Chaos, Solitons and Fractals,* **185** (2024). DOI: 10.1016/j.chaos.2024.115179

[20] C. Dong and M. Yang: A novel 4D memristor-based hyperchaotic system with hidden attractors: Dynamics, periodic orbits analysis, and DSP realization. *Chinese Journal of Physics,* 89 (2024). DOI: 10.1016/j.cjph.2024.04.003

[21] X. Shi, Y. Yang, X. Dai, C. Xiang and Y. Feng: Andronov–Hopf and Bogdanov–Takens bifurcations in a Filippov Hindmarsh–Rose system with switching policy for the slow variable. *Physica D: Nonlinear Phenomena,* **466** (2024). DOI: 10.1016/j.physd.2024.134217

[22] E. Abbasi and S. Jafari: Chaotic dynamics in X-ray free-electron lasers with an optical undulator. *Scientific Reports,* **14**(1). DOI: 10.1038/s41598-024-51891-1

[23] L. Zhang, Z. Li and Y. Peng: A hidden grid multi-scroll chaotic system coined with two multi-stable memristors. *Chaos, Solitons and Fractals,* **185** (2024). DOI: 10.1016/j.chaos.2024.115109

[24] A.N.N. Gilmolk and R.M. Aref: Lightweight image encryption using a novel chaotic technique for the safe internet of things. *International Journal of Computational Intelligence Systems,* **17**(1), (2024). DOI: 10.1007/s44196-024-00535-3

[25] I.A. Shepelev, A.V. Bukh and G.I. Strelkova: Anti-phase synchronization of waves in a multiplex network of van der Pol oscillators. *Chaos, Solitons and Fractals,* **162** (2022). DOI: 10.1016/j.chaos.2022.112447

[26] B. Ganesan and M. Annamalai: Anti-synchronization analysis of chaotic neural networks using delay product type looped-Lyapunov functional. *Chaos, Solitons and Fractals,* **174** (2023). DOI: 10.1016/j.chaos.2023.113898

[27] S. Vaidyanathan and A.T. Azar: *Backstepping Control of Nonlinear Dynamical Systems,* Academic Press, Cambridge, Massachusetts, USA, 2020.

[28] X. Liu, N. Li, C. Liu, J. Fu and H. Wang: Parameter tuning of modified adaptive backstepping controller for strict-feedback nonlinear systems. *Automatica,* **166** (2024). DOI: 10.1016/j.automatica.2024.111726

[29] S. Yan, J. Wang and L. Li: Analysis of a new three-dimensional jerk chaotic system with transient chaos and its adaptive backstepping synchronous control. *Integration,* **98** (2024). DOI: 10.2139/ssrn.4775234

[30] S. Yan, J. Wang, E. Wang, Q. Wang, X. Sun and L. Li: A four-dimensional chaotic system with coexisting attractors and its backstepping control and synchronization. *Integration,* **91**(2), (2023), 67–78. DOI: 10.1016/j.vlsi.2023.03.001